Pressure Induced Structural Phase Transitions in Pr_2CuO_4

H. Wilhelm, C. Cros[a], E. Reny[a], G. Demazeau[a] and M. Hanfland[b]

Département de Physique de la Matière Condensée, Université de Genève, Quai Ernest–Ansermet 24, 1211 Geneva 4, Switzerland
[a]Institut de Chimie de la Matière Condensée de Bordeaux, UPR-CNRS 9048, Avenue Dr. Albert Schweitzer 87, 33608 Pessac, France
[b]European Synchrotron Radiation Facility, B. P. 220, 38043 Grenoble, France

The influence of high pressure on the crystal structure of Pr_2CuO_4 (tetragonal Nd_2CuO_4-type) was studied at room temperature up to 37 GPa using synchrotron radiation. Upon increasing pressure a structural transformation into the T-structure (tetragonal K_2NiF_4-type) was observed at P_T = 15.1 GPa. A gradual distortion of the *T*-structure into the orthorhombic O-phase (*Cmca*) was found during pressure release in a certain pressure interval but eventually the initial T'-structure was recovered again. The pressure induced structural changes are discussed together with results on several members of the $La_{2-x}Nd_xCuO_4$ solid-solution. **[Keywords:** equation of state (EOS) – Pr_2CuO_4, phase transition – Pr_2CuO_4, Pr_2CuO_4, synchrotron radiation studies]

1. Introduction

La_2CuO_4 and Nd_2CuO_4 are the parent compounds of the hole– and electron–doped superconductors $La_{2-z}Sr_zCuO_4$ and $Nd_{2-y}Ce_yCuO_4$. $La_{2-z}Sr_zCuO_4$ is the simplest copper–oxide superconductor and its systematic study has revealed an evolution from an antiferromagnetic (AFM) insulator to a normal metal via a superconducting state ($0.07 \leq z \leq 0.24$; $T_c \approx 36$ K for $z = 0.15$ [1]). The AFM order is caused by the Cu–moments which are ordered below $T_N = 320$ K [2]. The crystal structure is orthorhombic (*Cmca*) and contains distorted [CuO_6] octahedra (Fig. 1). The CuO_2 planes are buckled to relieve compressive stress on them caused by the mismatch of (La,Sr)–O and Cu–O bonds. As z exceeds 0.21, a structural transition into the tetragonal K_2NiF_4 structure occurs (T–structure, $I4/mmm$, Fig. 1(c)) and simultaneously the superconducting transition temperature T_c decreases sharply [1,3]. Measurements on samples with $z \leq 0.18$ under hydrostatic pressure showed that T_c increases linearly with pressure but does not vary as soon as the tetragonal phase is induced by pressure [4,5]. This change in $\partial T_c/\partial P$ is believed to be related with the orthorhombic–tetragonal transition [3] and thus the maximum in T_c occurs when the CuO_2 planes are flat or almost flat. Furthermore, pressure experiments on $La_{2-z}Sr_zCuO_4$ ($z = 0.10$ and $z = 0.15$) have shown that T_c varies inversely with the tilt angle and is maximum in the tetragonal structure, i. e. with flat and square CuO_2 planes [6].

An interesting difference to the magnetic properties of the compounds mentioned so far is found for the parent compound of the electron–doped superconductors $R_{2-y}Ce_yCuO_4$ (R = Pr and Nd) [7]. In Nd_2CuO_4 (T'–structure, $I4/mmm$, Fig. 1(a)) several magnetic phases occur as the temperature is lowered or a magnetic field is applied. Furthermore, the magnetic moment of the Nd^{3+} is able both to interact with (next nearest) Cu–spins and to order spontaneously at low temperature (Ref. [8] and references therein). Below 30 K the Cu–moments are oriented antiferromagnetically along the a–axis as well as in the basal plane of the tetragonal structure. Along the c–axis adjacent Cu–spins are coupled ferromagnetically. The same order occurs for the Nd–sublattice below 5 K.

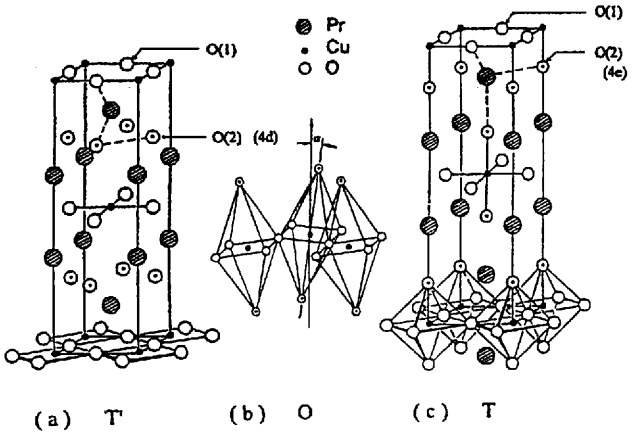

FIG. 1. Schematic view of the different crystal structures attained by Pr_2CuO_4 at different pressures. (a) The low pressure T'–phase ($I4/mmm$, Nd_2CuO_4–type), (b) the intermediate orthorhombic O–phase (*Cmca*, distorted K_2NiF_4–type), and (c) the high pressure T–phase ($I4/mmm$, K_2NiF_4–type).

Neighboring Nd– and Cu–spins are coupled ferromagnetically. In the $Nd_{1.85}Ce_{0.15}CuO_4$ superconductor the Cu–spins are not ordered but the Nd–sublattice shows the same magnetic order (below 1.2 K) as in Nd_2CuO_4 [9]. Thus the magnetic order coexists with superconductivity. In addition, heavy–fermion behavior below 1 K was found for a doping range $0.15 \leq y \leq 0.2$ [10]. This behavior probably arises from the combination of the strong coupling of the Nd and Cu moments and the Nd–Nd interaction.

Pressure experiments on Pr_2CuO_4 showed that similar spin re–orientations as in Nd_2CuO_4 can be induced by volume compression but T_N hardly changes [11]. The lat-

Science and Technology of High Pressure,
Proceedings of AIRAPT-17, edited by M.H. Manghnani, W.J. Nellis and M.F. Nicol, pp. 740–743, Universities Press, Hyderabad, India, 2000.

ter finding is quite different from that found for La_2CuO_4. Such a distinction can be caused by a different enhancement of inter-plane exchange coupling under pressure. If the pressure effects on T_N and T_c in both kind of superconductors (n- and p-doped) are related, then the AFM correlations might play an important role for superconductivity.

In the context of the above mentioned various physical ground states in combination with the structural transitions it is worthwhile to study in detail the pressure-induced structural changes of the Nd_2CuO_4 (T'-) structure attained by Pr_2CuO_4. This will deliver important information about the phase sequence, axis and volume compressibilities, and the pressure dependence of the Ln-O and Cu-O distances.

2. Experimental Details and Results

The polycrystalline sample of Pr_2CuO_4 was synthesized by a co-precipitation method. Stoichiometric amounts of oxides CuO and Pr_6O_{11} were separately dissolved in hot solutions of HNO_3, which were then cooled down to room temperature and diluted with water. The Pr^{3+} and Cu^{2+} solutions were poured simultaneously in a solution of potassium carbonate in excess. After decantation, the precipitate was filtered and carefully washed with water. After drying at 110°C and grinding, the resulting mixture was reacted twice at 850°C for 24 hours with an intermediate grinding. All the high temperature reactions and treatments were carried out under nitrogen atmosphere. The resulting products were identified by x-ray diffraction, using a conventional powder diffractometer (Cu-K_α and $\theta < 70°$).

The high pressure experiments were performed at ambient temperature using a membrane-type diamond anvil cell at the European Synchrotron Radiation Facility. Nitrogen served as pressure transmitting medium. The pressure was determined with the ruby luminescence technique [12] and the non-linear ruby pressure scale [13,14]. The x-ray powder diffraction spectra were recorded at the beamline ID09 at the ESRF. The high x-ray flux of the synchrotron combined with the image plate (size A3) provides a much better resolution than the technique used in the investigation reported in Ref. [15]. The diffraction images were collected at a wavelength of $\lambda = 0.46053$ Å ($E \approx 27$ keV) during 60s exposure time. The images were integrated with the program *fit2d* [16].

The structural parameters and interionic distances were obtained by Rietveld refinement [17] of the diffraction patterns in the range $3° < 2\theta < 23°$. The coexistence of two phases was taken into account by adjusting a phase fraction parameter. Furthermore, isotropic temperature factors were used. Those of the Pr and Cu atoms and those of the oxygen atoms were kept the same and these two parameters were refined independently. All refinements gave R_{wp} values between 2% and 6% depending on the pressure where the pattern was obtained. As diffraction lines of N_2 occurred they were refined too.

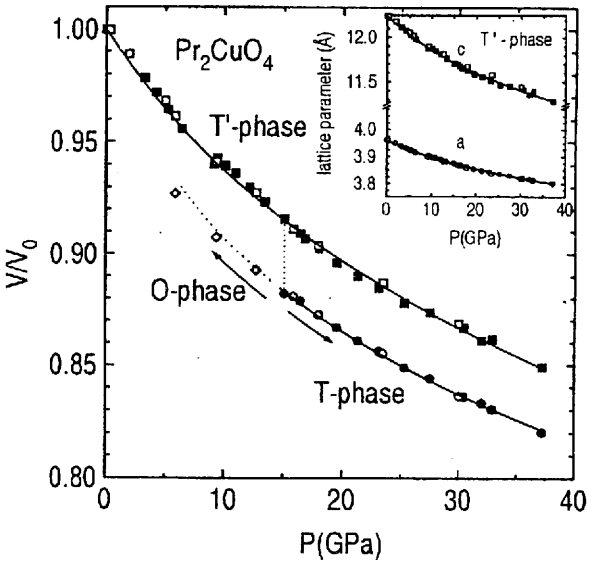

FIG. 2. Relative unit-cell volume V/V_0 of Pr_2CuO_4 versus pressure. The solid lines represent a fit of an EOS to the data. The low pressure T'-phase starts to transform gradually into the T-phase at $P_T = 15.1$ GPa. At the highest pressure reached ($P = 37.2$ GPa) still 50% of the T'-phase is present. During pressure release (open symbols) the orthorhombic O-phase (open diamonds) occurs. In the inset the pressure dependence of the lattice parameters of the T'-phase is shown.

The pressure dependence of the relative volume V/V_0 and the lattice parameters of Pr_2CuO_4 are shown in Fig. 2. The low pressure T'-phase is stable up to $P_T = 15.1$ GPa. At this pressure first signs of the high pressure T-phase were observed. The T-phase fraction increases with pressure but the pattern contained 50% of the low pressure T'-phase even at 37.2 GPa, the highest pressure reached in this experiment. Pressure release yielded the same structural parameters as upon increasing pressure (open symbols in Fig. 2). However, just below P_T the orthorhombic O-phase occurred in a small pressure interval (5.8 GPa $< P <$ 12.6 GPa). The initial T'-phase structure and lattice parameters were eventually recovered again at low pressure. The solid lines in Fig. 2 represent a fit of an equation of state (EOS) to the data. For the low pressure phase the Murnaghan EOS [18] gave B_0=126(2) GPa for the bulk modulus and B_0'=5.0(6) for its pressure derivative. The compressibilities of the lattice parameters were found to be $\kappa_a = \Delta a/a_0 = -2.0(1) \times 10^{-3}$ GPa^{-1} and $\kappa_c = \Delta c/c_0 = -3.7(2) \times 10^{-3}$ GPa^{-1}, with $a_0 = 3.9609(1)$Å and $c_0 = 12.2395(3)$Å, the lattice parameters at ambient pressure.

As can be seen in the inset of Fig. 2 the T'-structure is more compressible along the c-axis as along the a-axis. This behavior is intuitively obvious as the crystal structure is regarded (see Fig. 1). In the low pressure phase the Pr-Cu distance along the c-axis is rather long. Thus,

a compression along this direction is easier to achieve as in the (a,b)-plane, where the O(2) ions give rise to a strong electrostatic repulsion.

3. Discussion

The influence of high pressure on the T'-structure can be understood qualitatively in considering the coordination number of the rare earth ion and the density of the structure. As pressure is applied the density increases and a higher coordination number is favored. Hence the T'→T transition is very likely to occur. But to understand the stability of the different structures the bond-length matching between adjacent layers has to be considered. The stability of different structures can be evaluated from the tolerance factor t, defined by Goldschmidt [19] for the perovskite-structure: $t = (r_{Ln^{3+}} + r_{O^{2-}})/\sqrt{2}(r_{Cu^{2+}} + r_{O^{2-}})$, where $r_{Ln^{3+}}$, $r_{Cu^{2+}}$, and $r_{O^{2-}}$ are the ionic radii of the lanthanide, the copper, and the sixfold coordinated oxygen ions, respectively [19,20]. For the $La_{2-x}Nd_xCuO_4$ solid-solution the following phase diagram at normal conditions has been obtained [21,22]: (i) the T-structure exists for $0.99 \geq t \geq 0.88$, (ii) the O-structure is present for $0.88 > t \geq 0.865$, (iii) the T'-structure is stable for $0.865 > t \geq 0.83$, and (iv) for $0.83 > t$ a mixture of Ln_2O_3 and a new compound with the formula $Ln_2Cu_2O_5$ is found [22,23]. A special treatment of such a mixture at high pressure and high temperature has allowed to stabilize the T'-structure down to t=0.814 (for Ln=Tb, Dy, Ho, Er, Tm) [24].

In the T-structure compressive and tensile forces are present in the basal CuO_2 plane and along the c direction (Ln–O(2)), respectively. For La_2CuO_4, the Cu–O(1) distance (1.91 Å $\approx a/2$) is shorter than the sum of the ionic radii (2.13 Å, with $r_{Cu^{2+}} = 0.73$ Å and $r_{O^{2-}} = 1.40$ Å) leading to a compression. The two Cu–O(2) distances are significantly longer (2.46 Å, using $c = 13.15$ Å [22,25]). The tension is due to the fact that eight out of nine Ln–O distances are longer (≈ 2.64 Å for Ln–O(1) and ≈ 2.77 Å for Ln–O(2)) and only the distance between the lanthanide and the apical oxygen ($\approx$ 2.30 Å) is shorter than the sum of the ionic radii (2.62 Å, using $r_{La^{3+}} = 1.216$ Å). Both kinds of stresses are partially relieved by a cooperative tilting of the octahedra, resulting in the orthorhombic O-structure (i. e. the T → O transition).

In $La_{2-x}Nd_xCuO_4$ the average size of the lanthanide as well as the tolerance factor t decrease with Nd substitution. According to the definition of t and the average radius $r_{Ln^{3+}} = 0.5[(2-x)r_{La^{3+}} + xr_{Nd^{3+}}]$, with $r_{La^{3+}} = 1.216$ Å and $r_{Nd^{3+}} = 1.163$ Å [26], a linear relation between t and x exists. When the critical value $t = 0.865$ is reached, the O(2) ions move from the 4*e* sites of the O-structure (0,0,z; 0,0,-z) to the 4*d* sites $(0,\frac{1}{2},\frac{1}{4};\ \frac{1}{2},0,\frac{1}{4})$ of the T'-structure (see Fig. 1). The O → T' transition as a function of the average lanthanide ion size has been interpreted as optimization of the Ln–O distances [20–22]. The average Ln–O distance in the T'-structure is significantly shorter (2.51 Å instead of 2.64 Å) in the resulting fluorite-like arrangement (coordination number $CN(Ln^{3+}) = 8$) compared to the O-structure ($CN(Ln^{3+}) = 9$). Among the eight Ln–O distances in the T'-structure four are significantly shorter (2.32 Å, for Ln–O(2)) and four are longer (2.68 Å, for Ln–O(1)) than the sum of the ionic radii (2.51 Å). Therefore, a compression in the Ln–O(2) linkages is present. Furthermore, the oxygen ions at the 4*d* site are separated only by $a/\sqrt{2}$ (≤ 2.81 Å), which is very close to the sum of the ionic radii (2.80 Å). To diminish the O(2)–O(2) repulsion, the structure had to expand along the a- and b-axis. As a consequence the CuO_2-layers in the T'-structure are under tension.

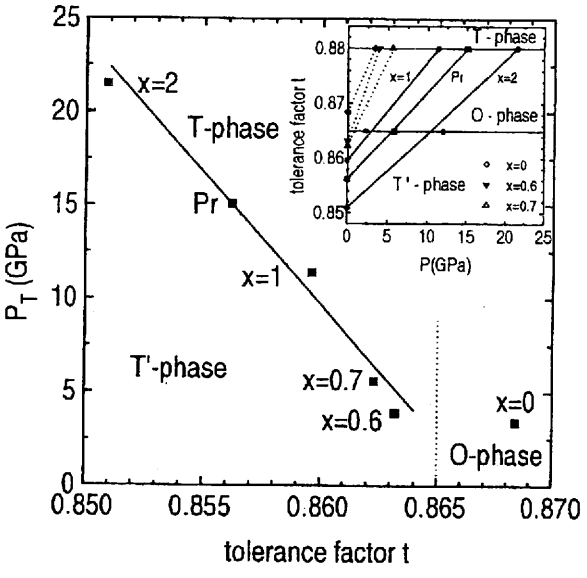

FIG. 3. Transition pressure P_T versus the tolerance factor t for Pr_2CuO_4 and several $La_{2-x}Nd_xCuO_4$ compounds [27 – 29]. The straight line separates the T'- and T-phase. Above $t = 0.865$ the orthorhombic O-phase is the stable low pressure phase. The point shown in this region represents La_2CuO_4 which transforms into the T-phase at 3.4 GPa. The tolerance factor t versus P_T is plotted in the inset. Points at the $t = 0.865-$ (0.88)-line represent the lowest pressures where the O-(T-)phase was observed.

The results of the high pressure studies on Pr_2CuO_4 can be well understood if the transition pressure P_T is plotted versus the tolerance factor t. Taking the ionic radius of Pr^{3+}, $r_{Pr^{3+}} = 1.179$ Å, the tolerance factor $t = 0.8562$ is obtained. In Fig. 3 the transition pressure versus the tolerance factor is shown for Pr_2CuO_4 and several members of the solid-solution $La_{2-x}Nd_xCuO_4$ [27–29]. We have chosen t as variable because it takes the Ln–O and Cu–O ionic bonding into account and gives an estimate of the structural stability. The t-values of the T'- and O-structure have been calculated using rare earth ions in a ninefold and copper and oxygen ions in a sixfold coordination. Fitting a linear $P_T(t)$-dependence (solid line in Fig. 3) to the data and extrapolating it down to

$P_T = 0$ GPa yields $t = 0.8669$. This value is only slightly higher than $t = 0.865$ which represents the border of stability of the T'–structure, indicated by the vertical line in Fig. 3.

An interesting insight in the phase sequence can be obtained if the tolerance factor is plotted versus pressure (inset Fig. 3). The symbols at ambient pressure are the tolerance factor of the various compounds at ambient pressure. The corresponding points at the borderline of the O– and T–phase ($t = 0.865$– and $t = 0.88$–line) represent the transition pressure P_T found for Pr_2CuO_4, several $La_{2-x}Nd_xCuO_4$ compounds [27–29], and La_2CuO_4 [30]. Assuming a linear $t(P)$–relation the $t(P = 0)$ and $t(P_T)$–points can be connected by a straight line. This immediately gives an intersection with the $t = 0.865$–line, representing the lower limit of the O–phase. The intersections for $x = 1$ and 2 as well as for Pr_2CuO_4 are very close to the points plotted at this line. They are the lowest pressure values where the O–phase was still observed in the diffraction patterns obtained during pressure release.

The fact that the intermediate O–phase is not observed during increasing pressure and the existence of a large T'– and T–phase domain (more than 25 GPa in the case of Pr_2CuO_4) is likely due to some hysteresis in the phase transitions, since the experiments were carried out at room temperature. This phenomenon is less pronounced during decreasing pressure, and the observed phase sequence T → O → T' shows clearly how pressure is able to tune the value of the tolerance factor t. The reversibility of the transition proves that the T–structure is not induced by a change in composition, but results only from the pressure effect. This is also confirmed by the crystal structure refinement of the synchrotron x–ray data [29].

4. Conclusion

The pressure–induced structural changes in Pr_2CuO_4 up to 37.2 GPa have been investigated by synchrotron radiation at room temperature. The ambient pressure T'–structure ($I4/mmm$, Nd_2CuO_4–type) starts to transform into the T–structure ($I4/mnm$, K_2NiF_4–type) at $P_T = 15.1$ GPa. However, the T'–phase fraction was still 50% at 37.2 GPa. During pressure release Pr_2CuO_4 attains in a certain pressure range the orthorhombic O–phase ($Cmca$, distorted K_2NiF_4–type) and transforms eventually into the initially T'–structure at low pressure. The structural changes are related to compressive stress in the Pr–O(2) linkages in the fluorite–like PrO_2–layers. In combination with previous results obtained on several members of the solid–solution $La_{2-x}Nd_xCuO_4$ it is found that the phase sequence T'→O→T can be well understood within the t–P_T diagram.

References

[1] B. Dabrowski, Z. Wang, K. Rogacki, J. D. Jorgensen, R. L. Hitterman, J. L. Wagner, B. A. Hunter, P. G. Radaelli, and D. G. Hinks, Phys. Rev. Lett. **76**, 1348 (1996).

[2] H. Casalta, P. Bourges, M. d'Astuto, D. Petitgrand, and A. Ivanov, Phys. Rev. B **57**, 471 (1998).

[3] J.-S. Zhou, J. B. Goodenough, H. Sato, and M. Naito, Phys. Rev. B **59**, 3827 (1999).

[4] N. Yamada and M. Ido, Physica C**203**, 240 (1992).

[5] J.-S. Zhou, H. Chen, and J. B. Goodenough Phys. Rev. B **49**, 9084 (1994).

[6] H. Takahashi, H. Shaked, B. A. Hunter, P. G. Radaelli, R. L. Hitterman, D. G. Hinks, and J. D. Jorgensen, Phys. Rev. B **50**, 3221 (1994).

[7] Y. Tokura, H. Takagi, and S. Uchida, Nature **337**, 345 (1989).

[8] N. M. Pyka, A. Metz, M. Loewenhaupt, R. van de Kamp, Physica B**241-243**, 865 (1998).

[9] J. W. Lynn, I. W. Sumarlin, S. Skanthakumar, W.-H. Li, R. N. Shelton, J. L. Peng, Z. Fisk, and S.-W. Cheong, Phys. Rev. B **41**, 2569 (1990).

[10] T. Brugger, T. Schreiner, G. Roth, P. Adelmann, and G. Czjek, Phys. Rev. Lett. **71**, 2481 (1993).

[11] S. Katano, N. Môri, H. Takahashi, T. Kobayashi, and J. Akimitsu, J. Phys. Soc. Jpn. **59**, 1928 (1990).

[12] G. J. Piermarini, S. Block, J. D. Barnett, and R. A. Forman, J. Appl. Phys. **46**, 2774 (1975).

[13] H. K. Mao, P. M. Bell, J. W. Shanner, and D. J. Steinberg, Appl. Phys. **49**, 3276 (1978).

[14] H. K. Mao, J. Xu, and P. M. Bell, J. Geophys. Res. **91**, 4673 (1986).

[15] W. H. Fietz, C. A. Wassilew, D. Ewert, M. R. Dietrich, H. Wühl, D. Hochheimer, and Z. Fisk, Phys. Lett. A **142**, 300 (1989).

[16] A.P. Hammersly, ESRF Internal Report EXP/AH/95-01(1995).

[17] A.C. Larson, GSAS manual, LAUR 86-748 (1986).

[18] F.D. Murnaghan, Proc. Natl. Acad. Sci. **30**, 244 (1944).

[19] V. M. Goldschmidt, Akad. Oslo I. Mater. Natur. **2**, 7 (1926).

[20] P. Ganguly and C. N. Rao, J. Solid State Chem. **53**, 193 (1984).

[21] A. Manthiram and J. B. Goodenough, J. Solid State Chem. **87**, 402 (1990).

[22] J. F. Bringley, S. S. Trail, and B. A. Scott, J. Solid State Chem. **86**, 310 (1990).

[23] N. Kimizuka, E. Takayama, and S. Horiuchi, J. Solid State Chem. **42**, 322 (1962).

[24] H. Okada, M. Takano, and Y. Takeda, Physica C **166**, 111 (1991).

[25] B. Grande, H. Müller–Buschbaum, and M. Schweitzer, Z. Anorg. Allg. Chem. **428**, 120 (1977).

[26] R. D. Shannon, Acta Crystallogr. Sect. A **32**, 751 (1976).

[27] H. Wilhelm, C. Cros, F. Arrouy, and G. Demazeau, J. Solid State Chem. **126**, 88 (1996).

[28] H. Wilhelm, C. Cros, E. Reny, G. Demazeau, and M. Hanfland, J. Mater. Chem. **8**, 2729 (1998).

[29] H. Wilhelm, C. Cros, E. Reny, G. Demazeau, and M. Hanfland, accepted for publication in J. Solid State Chem.

[30] J. Shu, J. Akella, J. Z. Liu, H. K. Mao, and L. Finger, Physica C **176**, 503 (1991).